Estimating the charm quark diffusion coefficient and thermalization time from *D* meson spectra at energies available at the BNL Relativistic Heavy Ion Collider and the CERN Large Hadron Collider

Francesco Scardina,[1,2] Santosh K. Das,[1] Vincenzo Minissale,[1,2] Salvatore Plumari,[1,2] and Vincenzo Greco[1,2]
[1]*Department of Physics and Astronomy, University of Catania, Via S. Sofia 64, 1-95125 Catania, Italy*
[2]*Laboratori Nazionali del Sud, INFN-LNS, Via S. Sofia 62, I-95123 Catania, Italy*
(Received 17 July 2017; published 17 October 2017)

We describe the propagation of charm quarks in the quark-gluon plasma (QGP) by means of a Boltzmann transport approach. Nonperturbative interaction between heavy quarks and light quarks have been taken into account through a quasiparticle approach in which light partons are dressed with thermal masses tuned to lattice quantum chromodynamics (lQCD) thermodynamics. Such a model is able to describe the main feature of the nonperturbative dynamics: the enhancement of the interaction strength near T_c. We show that the resulting charm in-medium evolution is able to correctly predict simultaneously the nuclear suppression factor, $R_{\rm AA}$, and the elliptic flow, v_2, at both Relativistic Heavy Ion Collider and Large Hadron Collider (LHC) energies and at different centralities. The hadronization of charm quarks is described by mean of an hybrid model of fragmentation plus coalescence and plays a key role toward the agreement with experimental data. We also performed calculations within the Langevin approach, which can lead to very similar $R_{\rm AA}(p_T)$ as Boltzmann, but the charm drag coefficient as to be reduced by about a 30% and also generates an elliptic flow $v_2(p_T)$ is about a 15% smaller. We finally compare the space diffusion coefficient $2\pi T D_s$ extracted by our phenomenological approach to lattice QCD results, finding a satisfying agreement within the present systematic uncertainties. Our analysis implies a charm thermalization time, in the $p \to 0$ limit, of about 4–6 fm/c, which is smaller than the QGP lifetime at LHC energy.

DOI: 10.1103/PhysRevC.96.044905

I. INTRODUCTION

The study of quantum chromodynamics (QCD) matter under extreme conditions of high temperatures is the primary purpose of ultrarelativistic heavy ion collisions that are being performed at the Relativistic Heavy Ion Collider (RHIC) and at the Large Hadron Collider (LHC). The energy deposited during the collisions produce a medium consisting of deconfined quarks and gluons called quark-gluon plasma (QGP) [1,2]. An essential role to characterize the QGP can be played by the hard probes created in the initial stage of the collisions. Among them heavy quarks (HQs), charm, and bottom, provide a very promising probe, since they travel through the expanding medium interacting with the light particles but their number is expected to be conserved due to the large M/T ratio. Therefore, HQ can probe the whole evolution of the QGP and produced out-of-equilibrium are expected to conserve memory of the history of the plasma evolution [3–7].

Moreover, HQ production can be calculated in next to leading order pQCD scheme and before the first experimental results it was expected that their interaction with the medium could be characterized by means of perturbative QCD, which led to the expectations of a small suppression of the spectra and a small elliptic flow. However, the first observations of nonphotonic electrons coming from heavy quark decays measured in Au+Au at $\sqrt{s_{\rm NN}} = 200$ GeV at RHIC [8–10] shown a surprisingly small $R_{\rm AA}$ and a quite large elliptic flow v_2, indicating a quite strong interactions between HQ and the medium which is substantially beyond the expectations from perturbative QCD [11–13]. These observations triggered many studies in which nonperturbative approach have been implemented. One of these approaches consists of including nonperturbative contributions [14] from the quasihadronic bound state with a subsequent hadronization by coalescence and fragmentation [15,16]. Other approaches make use of a pQCD framework supplemented by hard thermal loop (HTL) to evaluate Debye mass and running coupling constant [17,18]. Another efficient way is to use a quasiparticle approach in which nonperturbative effects are considered by introducing a thermal mass for the particle in the bulk, $m(T) \sim g(T)T$. A fit to lattice QCD (lQCD) thermodynamics allows to determine $g(T)$ [19,20]. All these models are based on collisional energy-loss which should be the dominant mechanism in the low momentum region of charm spectra [21–23], $p_T \lesssim 3 - 5M_{\rm HQ}$, while at higher momenta there is a consensus that radiative energy loss becomes dominant even if self-consistently collisional energy loss can never be discarded [23–26]. Furthermore, in the high-p_T region pQCD schemes have shown to be able to account for the observed suppression of the spectra [24,27,28] and some group obtained also a satisfying prediction for the elliptic flow [23,29].

In this paper, we will focus on the results of a quasiparticle model (QPM) for charm quarks. In Ref. [19] it is shown that the quasiparticle approach is able to reproduce the lattice QCD equation of state. The extracted coupling $g(T)$ appears to have a significant deviation from pQCD especially a $T \to T_c$. This leads to a weakly T dependent drag coefficient $\gamma(T)$ [30] at variance with pQCD with a constant coupling g or AdS/CFT where both predict a T^2 dependence drag coefficients. Such a feature of QPM has been found by other groups [20,31] that has also shown that the pattern remains quite similar even when quasiparticle widths (off-shell dynamics) are accounted for. It has been thoroughly studied in Ref. [30] for heavy quarks and also in Refs. [32,33] for the light sector that an interaction

increasing as the the temperature decreases is one of the key ingredient to generate a larger elliptic flow and thus reducing the tension between the R_{AA} and v_2 observed experimentally and calculated theoretically. This along with an hadronization via coalescence is also a main underlying reason of the early T-matrix approach applied at RHIC energy [13,14] and the following developments in Ref. [34]. In the present work, we employ the quasiparticle approach as discussed in Ref. [30].

The main difference in this work with respect to the results presented in Ref. [30] is the framework used to describe the heavy quark propagation based on a Boltzmann transport as well as the bulk evolution. Furthermore, while we already performed an analysis of such differences (in between Langevin and Boltzmann) for schematic cases like box calculations [35], here we present the results for AA collisions at both RHIC and LHC energies and different centralities. Furthermore, we also include here a fragmentation plus coalescence for heavy quark hadronization and moreover we discuss the difference entailed in terms of the spatial diffusion coefficient D_s and compare them to lattice QCD results.

The article is organized as follows. In Sec. II, we discuss briefly the Boltzmann transport equation and the quasiparticle approach for HQs. In Sec. III, we describe the hybrid model of fragmentation and coalescence to consider the hadronization process of heavy quarks into heavy flavor mesons in QGP. Section IV is devoted to the comparison between the simulation results with experimental results at different colliding energy and different centralities. In Sec. V, we discuss the heavy quark transport coefficient obtained within the present approach. Section VI contains a summary and some concluding remarks.

II. TRANSPORT EQUATION FOR CHARM QUARKS IN THE QGP

The evolution of the charm quark distribution function is obtained solving the relativistic Boltzmann transport equations [35,36] for charm quarks scattering in a bulk medium of quarks and gluons:

$$\begin{aligned} p^\mu \partial_\mu f_Q(x,p) &= \mathcal{C}[f_q, f_g, f_Q](x,p), \\ p_q^\mu \partial_\mu f_q(x,p) &= \mathcal{C}[f_q, f_g](x_q, p_q), \\ p_g^\mu \partial_\mu f_g(x,p) &= \mathcal{C}[f_q, f_g](x_g, p_g), \end{aligned} \tag{1}$$

where $f_k(x,p)$ is the on-shell phase space one-body distribution function for the k parton and $\mathcal{C}[f_q, f_g, f_Q](x,p)$ is the relativistic Boltzmann-like collision integral and the phase-space distribution function of the bulk medium consists of quark and gluons entering the equation for charm quarks as an external quantities in $\mathcal{C}[f_q, f_g, f_Q]$. We assume that the evolution of f_q and f_g are independent of $f_Q(x,p)$ and discard collisions between heavy quarks, which is by far a solid approximation. We are interested in the evolution of the HQ distribution function $f_Q(x,p)$. The evolution of the bulk of quark and gluons is instead given by the solution of the other two transport equations where the $\mathcal{C}[f_q, f_g]$ is tuned to a fixed $\eta/s(T)$, as discussed in detail in Ref. [37]. This is, however, quite equivalent to a modeling where the bulk is given by viscous hydrodynamics.

The collision integral for heavy quarks is given by

$$\begin{aligned} \mathcal{C}[f_Q] = \frac{1}{2E_1} \int \frac{d^3p_2}{2E_2(2\pi)^3} \int \frac{d^3p_1'}{2E_{1'}(2\pi)^3} \\ \times [f_Q(p_1') f_{q,g}(p_2') - f_Q(p_1) f_{q,g}(p_2)] \\ \times |\mathcal{M}_{(q,g)+Q}(p_1 p_2 \to p_1' p_2')|^2 \\ \times (2\pi)^4 \delta^4(p_1 + p_2 - p_1' - p_2'), \end{aligned} \tag{2}$$

where $\mathcal{M}_{(q,g)+Q \leftrightarrow (q,g)+Q}$ corresponds to the transition amplitude of the HQ scatterings. To solve the collision integral it is necessary to evaluate the scattering matrix of the microscopical process. In the present paper, this is done in the framework of a quasiparticle model as described in the following.

The evolution of the QGP bulk given by an approach in which we gauge the collision integral to the wanted η/s as described in Refs. [37–40]. In this way, we are able to simulate the dynamical evolution of a fluid with specified η/s by means of the Boltzmann equation. In the case considered here, we have more specifically employed a bulk with massive quarks and gluons that provide the possibility to have a softening of the equation of state with a decreasing speed of sound when the cross over region is approached. Within this approach, we describe the evolution of a system that dynamically has approximatively the lQCD equation of state [41]. As shown in Ref. [42], within this approach we recover universal features of hydrodynamics and it permits to study the impact of $\eta/s(T)$ on observables like $v_n(p_T)$ in analogy to what is done within hydrodynamical simulations [43–46].

The numerical solution of the Boltzmann equation is obtained by means of the test particle method to map the one body distribution and we divide the space in a three-dimensional grid. For being in a regime of convergence we employ a number of test particle per real particle of 400, which we have verified allow to give a good convergence also for differential observables like $v_2(p_T)$. More generally it has been checked that the numerical solution of the Boltzmann equation for HQs leads to the Boltzmann-Juttner equilibrium distribution function in all the relevant momentum range.

The key role is certainly played by the scattering matrix $\mathcal{M}_{(q,g)+Q \leftrightarrow (q,g)+Q}$ that is the kernel of the interaction that allows also to calculate the drag and diffusion transport coefficients. The ingredient of the quasiparticle model are the thermal masses: $m_g^2(T) = 3/4 g^2(T) T^2$, $m_{u,d}^2(T) = 1/3 g^2(T) T^2$ and $m_{u,d}^2(T) - m_{0s}^2 = 1/3 g^2(T) T^2$. The parametrized form of the strong coupling constant $g(T)$ is evaluated by making a fit of the energy density obtained by lattice QCD calculations and in our case has been parametrized as

$$g^2(T) = \frac{48\pi^2}{(11N_C - 2N_f) \ln\left[\lambda\left(\frac{T}{T_c} - \frac{T_s}{T_c}\right)\right]^2}, \tag{3}$$

where $N_c = N_f = 3$, $\lambda = 2.6$, and $T_s/T_c = 0.57$. It has been shown in Ref. [19] that QPM is able to reproduce with good accuracy the lattice QCD pressure and interaction measure $T^\mu_\mu = \epsilon - 3P$. The main feature of this approach is that the resulting coupling is significantly stronger than the one coming from pQCD running coupling, particularly as $T \to T_c$. The evaluation of the scattering matrix $\mathcal{M}_{(q,g)+Q \leftrightarrow (q,g)+Q}$ is then

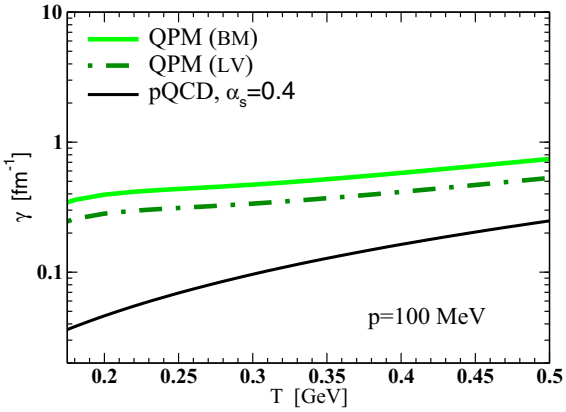

FIG. 1. Drag coefficients as a function of temperature obtained within the Boltzmann transport approach and Langevin dynamics to describe the same experimental data (shown in Fig. 4).

performed considering the leading-order diagram with the effective coupling $g(T)$ that leads to effective vertices and a dressed massive gluon propagator for $qQ \leftrightarrow qQ$ and massive quark propagator for $gQ \leftrightarrow gQ$ scatterings. The detail of the calculations for all u,t,s channels and their interferences is quite long even if proceed along a standard procedure and can be found in Ref. [47], where also a comparison with the massless case and the massive, including collisional widths, is presented.

In Fig. 1 we show the behavior of the drag coefficient γ with temperature in QPM by solid line. Such a drag is evaluated with the same scattering matrix $\mathcal{M}_{(q,g)+Q\leftrightarrow(q,g)+Q}$ driving the Boltzmann transport. By dotted line we show the same coefficient that is rescaled to describe the same $R_{\rm AA}(p_T)$, as the one obtained with Boltzmann dynamics but with the Langevin dynamics; see Fig. 4 and the related discussion. In fact, as first observed in Ref. [35], we need a smaller drag coefficient in Langevin dynamics to describe nearly the same experimental results than the Boltzmann transport approach. In the same figure, we have also included for comparison a standard LO-pQCD calculation with a constant coupling. This allows us to have an indication of the enhancement for the drag coefficient with respect to the LO pQCD to describe the experimental data. Moreover, we notice that QPM has a weaker temperature dependence of the drag coefficient which is one of the key ingredient for a simultaneous description of heavy quark $R_{\rm AA}(p_T)$ and v_2. This has been discussed in Ref. [30], but within a Langevin and not with a Boltzmann approach and not including the impact of coalescence; see Sec. IV.

The physics behind the different temperature dependence of QPM with respect to pQCD is in the increase of the non perturbative dynamics as the temperature decrease that in a QPM is induced by the fit to the lQCD thermodynamics. The former implies a coupling $g(T)$, which increase as $T \to T_c$ in a way that nearly compensates the decrease of the density resulting in a quite weak temperature dependence of the drag coefficient.

For a constant coupling and massless particles, the drag γ would go like $1/T^2$, solid black line in Fig. 1, with the strong decrease mainly driven by the decrease of the bulk density scatterers that is proportional to $1/T^3$. The same T dependence appears in AdS/CFT because also in such a case the strength of the interaction, the coupling to the medium, is not temperature dependence. Of course, however, in such a case the absolute value is much larger of about one order of magnitude with respect to the pQCD one; see also Fig. 12.

III. HADRONIZATION FOR CHARM QUARKS VIA COALESCENCE AND FRAGMENTATION

Hadronization dynamics plays an important role in determining the final spectra and therefore the $R_{\rm AA}(p_T)$ and $v_2(p_T)$ in both the light and heavy quark sector [13,15,16,48]. In particular, for heavy quarks it is generally expected that a coalescence mechanism is in action especially at low and intermediate p_T. We consider here a hybrid model of coalescence plus fragmentation discussing in detail its impact on both $R_{\rm AA}$ and v_2.

In our approach the hadronization hypersurface is determined by the isothermal surface of the bulk dynamics, which means that is determined stopping collisions between the light particles and the heavy quarks when the temperature of a cell drops below the critical temperature that has been fixed to T=155 MeV.

The contribution to hadronization due to coalescence is evaluated according to

$$\frac{d^2N_M}{dP_T^2} = g_M \int \prod_{i=1}^{2} \frac{d^3p_i}{(2\pi)^3 E_i}\, p_i \cdot d\sigma_i \; f_{q_i}(x_i,p_i) \times f_M(x_1-x_2,p_1-p_2)\delta^{(2)}(P_T - p_{T,1} - p_{T,2}), \tag{4}$$

where $d\sigma_i$ denotes an element of a spacelike hypersurface, g_M is the statistical factor to form a colorless hadron from quark and antiquark with spin 1/2. f_{q_i} are the quark (antiquark) distribution in phase space. f_M is the Wigner function and describes the spatial and momentum distribution of quarks in the D meson.

In the Greco-Ko-Levai (GKL) approach [16] for a heavy meson the Wigner function is taken as a Gaussian of radius Δ_x in the coordinate and Δ_p in the momentum space, these two parameters are related by the uncertainty principle $\Delta_x\Delta_p = 1$,

$$f_M(x_1,x_2;p_1,p_2) = 8\exp\left(x_r^2/2\Delta_x^2\right)\exp\left(p_r^2/2\Delta_p^2\right), \tag{5}$$

where the relative coordinates $x_r = x_1 - x_2$ and $p_r = p_1 - p_2$ are the quadrivectors for the relative coordinates. A pattern confirmed by all the groups, despite differences in the details, is that an hadronization by coalescence is dominant at low momenta [17,23,31,34,49,50], since the early work in Refs. [13,15]. We determine the width parameter Δ_p by requiring that the mean square charge radius of D^+ meson is $\langle r^2\rangle_{ch} = 0.43$ fm according to quark model. Given that for our wave function,

$$\langle r^2\rangle_{ch} = \frac{3}{2}\frac{Q_1m_2^2 + Q_2m_1^2}{(m_1+m_2)^2}\frac{1}{\Delta_p^2}, \tag{6}$$

with $Q_1 = +2/3$ and $Q_2 = +1/3$, we find $\Delta_p = 0.283$ GeV. We also include the D^* resonant states suppressed according

to the statistical thermal weight with respect to the ground state.

We compute the coalescence probability for each charm quark in the phase space point $(\vec{x},\tau,\vec{p})$ and then assign a probability of fragmentation as $P_{\rm frag}(\vec{x},\tau,\vec{p}) = 1 - P_{\rm coal}(\vec{x},\tau,\vec{p})$. Therefore, the charm distribution function undergoing fragmentation is evaluated convoluting the momentum of heavy quarks, which do not undergo coalescence with the Peterson fragmentation function [51],

$$f(z) \propto \frac{1}{\left[z\left[1-\frac{1}{z}-\frac{\epsilon_c}{1-z}\right]^2\right]}, \tag{7}$$

where $z = p_D/p_c$ is the momentum fraction of the heavy meson fragmented from the heavy quark and ϵ_c is a free parameter to fix the shape of the fragmentation function. As discussed in the next section the ϵ_c parameter will be determined assuring that the available data on D meson production in pp collisions are well described by a fragmentation hadronization mechanism. Finally, given the momentum distribution of the charm quarks obtained solving the Boltzmann equation the momentum distribution of D meson is calculated summing up the D meson spectrum obtained via coalescence with the one from fragmentation.

IV. COMPARISON TO THE EXPERIMENTAL OBSERVABLES

We present in this section the comparison of the results we get for the nuclear modification factor $R_{\rm AA}$ and for the elliptic flow v_2 with the experimental data. We calculate the nuclear suppression factor, $R_{\rm AA}$, as the ratio of our initial heavy meson distribution at $t = \tau_i$ and final heavy meson distribution at $t = \tau_f$ as

$$R_{\rm AA}^{c,D}(p_T) = \frac{f_{c,D}(p_T,\tau_f)}{f_{c,D}(p_T,\tau_i)}, \tag{8}$$

where $f_{c,D}(p_T,\tau_f)$ indicates the momentum distribution already integrated in the r space and in the rapidity range $|y_z| \leqslant 0.5$ for charm or D mesons. The $f_{c,D}(p_T,\tau_i)$ is the same distribution we employ for pp collisions, and that is shown in Figs. 2 and 3; see discussion below. However, we note that at LHC where the shadowing effect is expected to be large [52], we have also considered the case where in AA we start from an initial distribution function that is not the $f_c(p_T,\tau_i)$ that goes in the denominator of Eq. (8) but is given by

$$f_c^{SW}(p_T,\tau_i) = f_c(p_T,\tau_i) * S(p_T), \tag{9}$$

where the shadowing function $S(p_T)$ is a parametrization of EPS09 [52,53], already integrated in the pertinent rapidity region and over the r space.

In $p+p$ collisions, we convoluted the charm quarks distribution according to the fixed order + next-to-leading log (FONLL) calculations, taken from Refs. [55,56] with the Peterson fragmentation function [51] to obtain the D meson spectra. As mentioned, the free parameter ϵ_c in the fragmentation function, in Eq. (7), has been fixed by comparison to the D^0 meson production in $p+p$ collisions at RHIC energy as measured by STAR [54]. With $\epsilon_c = 0.006$ we obtain the spectrum shown in Fig. 2 by solid line. In Fig. 3, we show D^0 and D^+ meson spectra in $p+p$ collisions at LHC energy by solid black and light red lines, obtained with ϵ_c=0.02, and compare to the experimental results [53] that is an extrapolation from 7 to 2.76 TeV. With this initial conditions for charm distribution function and their fragmentation function we proceed to evaluate the D mesons spectra in heavy-ion collisions at RHIC and LHC.

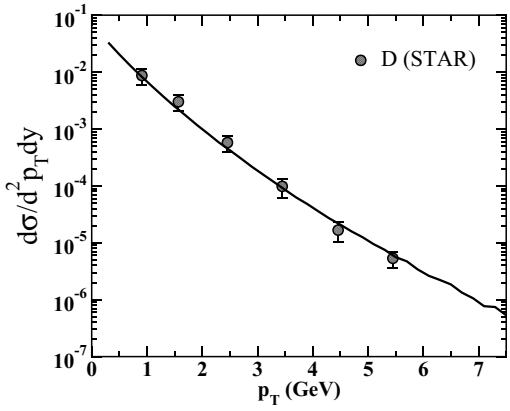

FIG. 2. The p_T distribution of D mesons, obtained from the fragmentation of charm quarks in $p+p$ collisions, are compared with the experimental data from the STAR Collaboration, taken from Ref. [54].

For $Au+Au$ collisions at $\sqrt{s} = 200$ AGeV, the initial conditions for the bulk in the r space are given by the standard Glauber condition, while in the p space we use a Boltzmann-Juttner distribution function up to a transverse momentum $p_T = 2$ GeV and at larger momenta mini-jet distributions as calculated by pQCD at NLO order [16]. The initial maximum temperature at the center of the fireball is $T_0 = 345$ MeV and the initial time for the simulations is $\tau_0 = 0.6$ fm/c, as commonly assumed in hydrodynamical

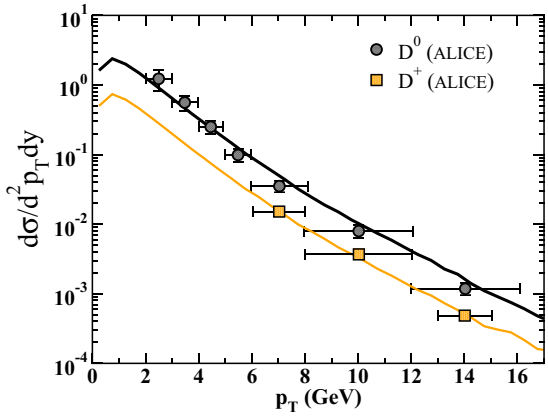

FIG. 3. The p_T distribution of D^0 and D^+ mesons, obtained from the fragmentation of charm quarks in $p+p$ collisions, are compared with the experimental data from the ALICE Collaboration,taken from Ref. [53]. The experimental points are an extrapolation from 7 to 2.76 TeV.

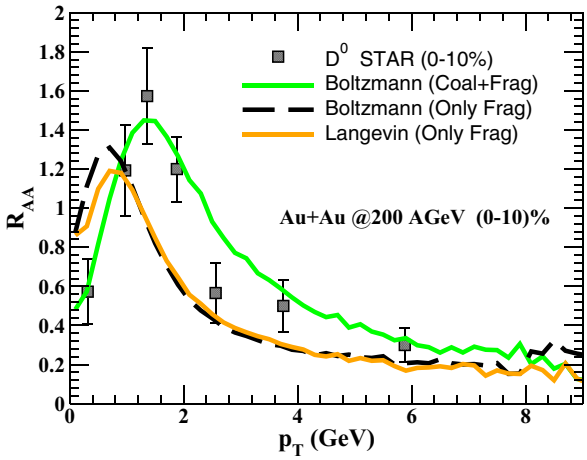

FIG. 4. D meson $R_{\rm AA}$ in $Au + Au$ collisions at $\sqrt{s} = 200$ AGeV and centrality 0–10% compared to STAR data. Experimental data has been taken from Ref. [58].

simulation [43,44,46,57], which is about corresponding to the $\tau_0 \cdot T_0 \sim 1$ criteria. In our calculation, quarks and gluons are massive to reproduce the lattice QCD equation of state, as mentioned in Sec. II. In the p space the charm quarks are distributed according to the FONLL calculations, taken from Refs. [55,56]. In the coordinate space HQ are distributed according to number of binary nucleon-nucleon collisions ($N_{\rm coll}$), corresponding to a constant cross section $\sigma_{\rm NN} = 40$ mb at RHIC and a$\sigma_{\rm NN} = 72$ mb at LHC.

The dynamical evolution of the bulk is constrained by an $\eta/s = 1/4\pi$, as discussed in Sec. II, in such way that the model reproduces the experimental data on the bulk spectra and elliptic flow [37,40]. When the system reaches locally the critical temperature the one body distribution functions of heavy quark are frozen and used to get the momentum distribution. This allows us to evaluate the nuclear modification factor and the elliptic flow of the D mesons by means of the hadronization model described in the previous section.

In Fig. 4, the $R_{\rm AA}(p_T)$ as a function of p_T in $Au + Au$ collisions at $\sqrt{s} = 200$ AGeV for centralities 0–10% that we obtained within our model calculation is depicted and compared with the experimental data measured at RHIC energy [58]. In this figure, we indicate the impact of coalescence on $R_{\rm AA}$ showing the $R_{\rm AA}$ we obtain considering only fragmentation (dashed line) along with the results obtained including the coalescence mechanism plus fragmentation (green solid line). We observe that the coalescence implies an increasing of the $R_{\rm AA}$ for momenta larger than 1 GeV, thus a reduction of the suppression. This is due to the hadronization mechanism which implies that a D mesons from coalescence of one light quark and a charm quark get a momentum kick with respect to the D mesons obtained from fragmentation that on the contrary has a reduced momentum with respect to the original quark according to ϵ_c in Eq. (7). This along with the fact that charm spectrum decreases with p_T implies that the final spectrum of D meson does not scale with the spectrum of the original charm. An increasing in the number of particle in the region of $p_T > 1$ GeV is observed. At larger momenta, see Fig. 6, fragmentation becomes anyway the dominant mechanism of hadronization. Such a decrease of coalescence impact that appears naturally in our model seems to be necessary to describe the p_T dependence observed experimentally. It has to be mentioned here that the trend of the experimental data at low p_T supports also the coalescence as the mechanism of heavy quark hadronization. Heavy quark hadronization only fragmentation could not describe the marked low p_T bump of the experimental data. We notice that for the collisions at RHIC we have not included a shadowing effect. This does not mean that there is no shadowing for heavy quarks but just that at RHIC within the experimental data uncertainties it does not appear as necessary its inclusion for a satisfying description of data at variance with respect to the LHC case that we discuss in the following. This is also in good agreement with recent calculations in Ref. [82].

It is shown in Ref. [35] that a nonnegligible difference arises between the Langevin and the Boltzmann approach to describes the HQ momentum evolution in QGP. In the present study at RHIC, we evaluate the $R_{\rm AA}(p_T)$ in $Au + Au$ collisions at $\sqrt{s} = 200$ AGeV within the Langevin dynamics for the centralities 0–10% and compare the results obtained within the Boltzmann transport approach. For the details of the Langevin simulations of HQ dynamics in QGP, we refer to Refs. [30,35,59]. In Fig. 4, we show the variation of $R_{\rm AA}(p_T)$ obtained within the Langevin dynamics using only fragmentation as the hadronization mechanism and compare the results obtained within the Boltzmann transport approach. As shown in Fig. 4, we can obtain a very similar $R_{\rm AA}(p_T)$ within both the Langevin dynamics as well using Boltzmann transport approach. However, the drag coefficient needed to predict a similar $R_{\rm AA}(p_T)$ within both the approach has to be rescaled down by about 30% as shown in Fig. 1. On the other hand, it is noteworthy that once the drag coefficient is rescaled by a constant (momentum independent factor) the prediction for $R_{\rm AA}(p_T)$ is nearly identical in quite a large range of p_T. An additional comment is, however, necessary. As discussed in Ref. [35] for some ideal case, the comparison of a Langevin dynamics with a Boltzmann one depends also on the way fluctuation-dissipation theorem (FDT) is implemented. We report here the case in which Langevin and Boltzmann are more similar. This occurs when the drag $\gamma(T, p_T)$ is evaluated from the scattering matrix while the diffusion coefficient are determined as $B_L = B_T = TE\gamma$. As known there are other possible choice which would lead in general to larger differences with respect to the Boltzmann dynamics; see Ref. [35].

Using the same interaction, as in Fig. 4, within Boltzmann transport approach, we proceed to compare the results at RHIC for a different centrality class as well as at LHC colliding energy. In Fig. 5, we shown the $R_{\rm AA}$ as a function of p_T in $Au + Au$ collisions at $\sqrt{s} = 200$ AGeV for centralities 10–40% and compared with the experimental data measured at RHIC energy [58]. By black dashed line the results obtain within only fragmentation and the green solid line obtained with fragmentation plus coalescence. In this centrality also we are getting reasonable agreement with the experimental data again, once the coalescence is included along with the fragmentation as the hadronization mechanism.

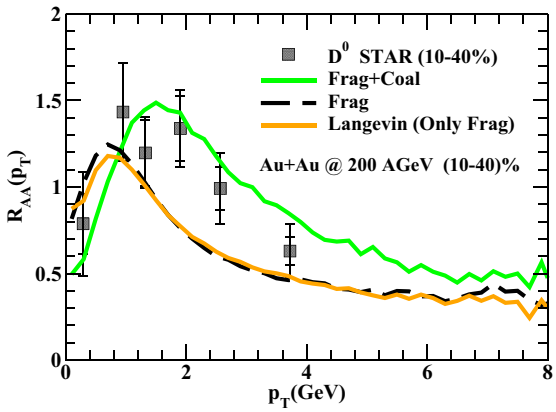

FIG. 5. D meson $R_{\rm AA}$ in $Au + Au$ collisions at $\sqrt{s} = 200$ AGeV and centrality 10–40% compared to STAR data. Experimental data has been taken from Ref. [58].

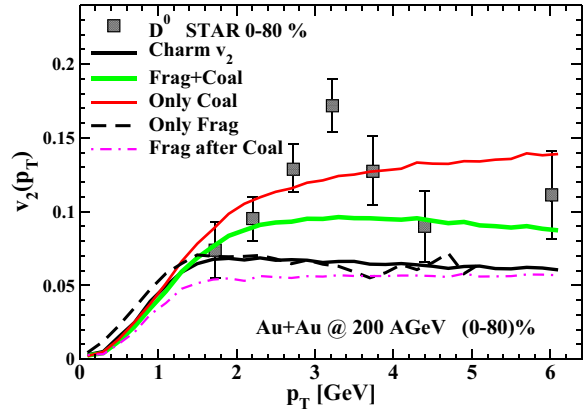

FIG. 7. D meson elliptic flow in $Au + Au$ collisions at $\sqrt{s} = 200$ AGeV and centrality 0–80% compared to STAR data. Experimental data has been taken from Ref. [61].

In Fig. 6 the probability of a charm hadronizing to a D mesons (D^0, D^+, D^{*0}, D^{+*}) through coalescence is depicted as a function of p_T. The charm quark hadronization probability to all hadrons, i.e. including charm baryons, is set to one in the $p \to 0$ limit, as usually done by several groups [21,31,34,60]. The hadronization probability decreases with momentum as the coalescence probability involves the product of two distribution functions that are decreasing with p_T. We found at LHC energy the coalescence probability is only marginally smaller than RHIC due to the harder charm quark distribution at LHC than RHIC.

In Fig. 7 are depicted the results for the elliptic flow as a function of momentum in $Au + Au$ collisions at $\sqrt{s} = 200$ AGeV for $b = 8\ fm$ that on average corresponds to the centrality 0–80%. We show explicitly the different contributions allowing a direct access to the role played by initial charm v_2 and by coalescence and fragmentation. The black line indicates the elliptic flow we get for the charm quark, obtained within the Boltzmann transport approach, without considering any hadronization mechanism, while the dashed black line indicates the v_2 for D mesons that we obtain considering only the fragmentation as hadronization mechanism. We observe that the v_2 is similar in the two cases with a little shift in the low momentum for the D meson case. This is because the fragmentation implies that the D mesons v_2 at a given transverse momentum is the result of the fragmentation of a charm quark v_2 with a slightly larger transverse momentum.

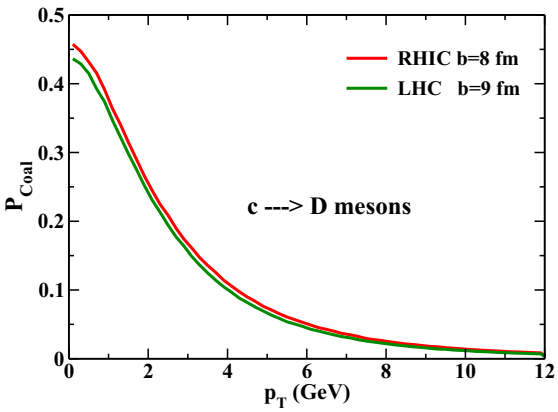

FIG. 6. Coalescence probability for a charm going to one of the mesons (D^+, D^0, D^{*0}, D^{+*}) as a function of transverse momentum at RHIC and LHC.

If coalescence plus fragmentation mechanism is included for the hadronization, the v_2 of the D mesons increases with respect to the elliptic flow of charm quarks by about a 30%, solid green line in Fig. 7. This is because the D meson is the result of the coalescence of a charm quark and a light quark and thus the D mesons anisotropy in momentum space reflect both the heavy quark and light quark anisotropies in momentum space. The solid red line shows the v_2 of D mesons produced only via coalescence. As expected, the v_2 developed only coalescence is larger than the v_2 developed due to coalescence plus fragmentation. It can even lead to an increase of about a factor of two at $p_T > 2$ GeV. This is due mainly due to the large v_2 of light quarks with respect to charm. The solid magenta line indicates the elliptic flow produced by the fragmentation of charm once also coalescence has been switched on. In this case, the elliptic flow is smaller with respect to that obtained when fragmentation is the only hadronization mechanism, indicated by dashed double dotted line. This last result is an indirect consequence of the phase space selection implicit in the coalescence mechanism that favors the quark pairs that are more correlated and hence those having momenta closer to the collective flow direction have a large coalescence probability. The ensemble of charm quarks left over from the coalescence process have a smaller $v_2(p_T)$ than the one of all the charm quark before hadronization. This is the reason why the v_2 is small for D mesons fragmented after coalescence than the D meson formed when only fragmentation is considered.

We have seen in Figs. 4 and 5 that rescaling the interaction by about a 30% Langevin gives results very similar to a Boltzmann dynamics. We extend here the comparison to elliptic flow showing in Fig. 8 a comparison with the $v_2(p_T)$ obtained in Langevin simulations. Langevin dynamics generates about a 15% smaller elliptic flow at charm level which propagates also to the elliptic flow of single electrons from D mesons decay,

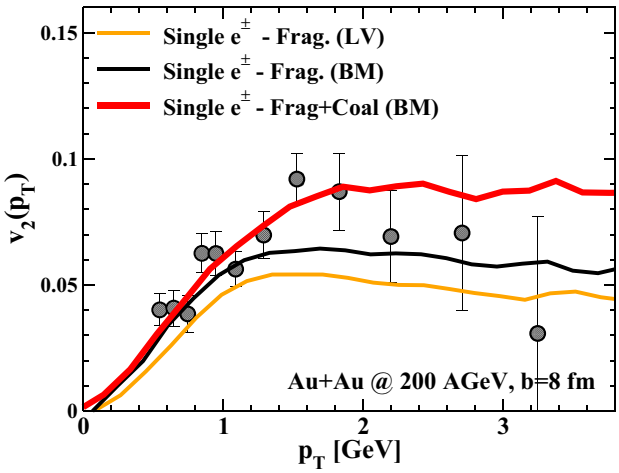

FIG. 8. Single electron elliptic flow in $Au + Au$ collisions at $\sqrt{s} = 200$ AGeV in minimum bias compared to PHENIX data. Experimental data has been taken from Ref. [8].

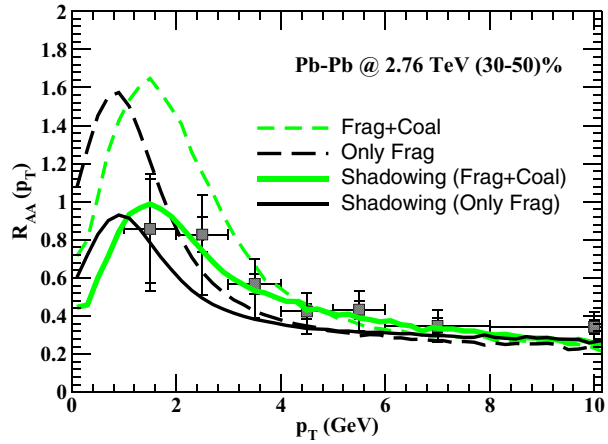

FIG. 10. D meson $R_{\rm AA}$ in $Pb + Pb$ collisions at $\sqrt{s} = 2.76$ ATev and centrality 30–50% compared to ALICE data. Experimental data has been taken from Ref. [62].

shown in Fig. 9 by orange solid line along with the one of the Boltzmann case in black solid line. We mention that if for the Langevin case the interaction is not scaled down by 30% then the elliptic flow would be quite similar to the Boltzmann case, but the corresponding $R_{\rm AA}(p_T)$ would be quite smaller. We also show in Fig. 8 by solid thick red line our prediction for the single $e^{\pm}$ with the Boltzmann dynamics and hadronization by coalescence plus fragmentation that indeed is in good agreement with the experimental data from PHENIX. We just remind experimental single electrons come also from B meson decay and are expected to be significant for $p_T > 2$ GeV.

Using the same QPM drag coefficient as at RHIC, we have carried out a simulation of $Pb + Pb$ collisions at $\sqrt{s} =$ 2.76 ATeV for centralities 0–10% and 30–50%. In this case the initial maximum temperature in the center of the fireball is $T_0 = 490$ MeV and the initial time for the simulations is $\tau_0 \sim 1/T_0 = 0.3$ fm/c. In Fig. 9 the results for the $R_{\rm AA}$ at 0–10% centrality are depicted with only fragmentation and

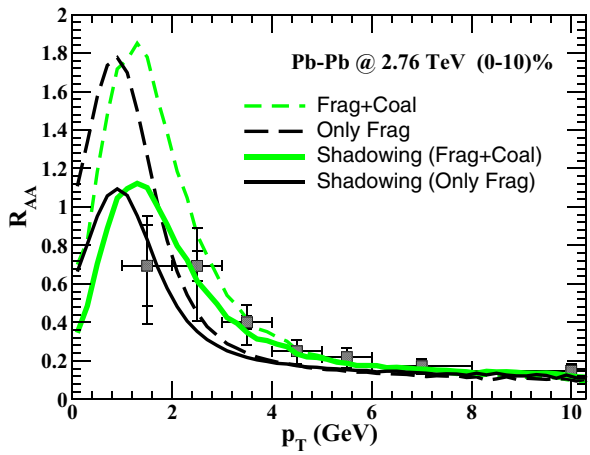

FIG. 9. D meson $R_{\rm AA}$ in $Pb + Pb$ collisions at $\sqrt{s} = 2.76$ ATev and centrality 0–20% compared to ALICE data. Experimental data has been taken from Ref. [62].

fragmentation plus coalescence. In LHC, as of RHIC, we observe that the coalescence implies an increasing of the $R_{\rm AA}$ for momenta larger than 1 GeV. As evident, the effect of coalescence is less significant at LHC energy than at RHIC energy. This is because the effect of coalescence depends on the slope of the charm quark momentum distribution. For a harder charm quark distribution the gain in momentum reflects in a smaller increase of the slope spectrum, instead if the charm quark distribution decreases faster in momentum then the same momentum gain due to coalescence will result in a stronger increase of the spectrum. For a harder charm quark distribution, like at LHC energy, the impact of coalescence is therefore less pronounced, despite still we see that it leads to a better agreement with the experimental data also at LHC.

In Fig. 10, we present $R_{\rm AA}$ with respect to p_T for more peripheral collisions at 30–50%. We see a similar coalescence effect as in central collision and also in this case it allows a much better description of the experimental data when the shadowing is included. Indeed the data and our calculations seem to clearly show a shadowing effect in agreement with EPS09 [52] within the still large uncertainties at low p_T in the data. In Fig. 11, as expected, coalescence increase both the $R_{\rm AA}$ and v_2 and bring the results close to the data, toward a simultaneous description of heavy meson $R_{\rm AA}$ and v_2. At LHC energy also, the v_2 is significantly smaller for D mesons fragmented after coalescence than the D meson produced due to only fragmentation. We notice the very recent data [63] are an average of the measurements in $Pb + Pb$ at $\sqrt{s} = 5.02$ ATeV that we include here because it is the only available data on v_2 with a not-too-large uncertainty. On the other hand, in our modeling the results increasing the beam energy up to 5.02 ATeV would only affect the elliptic flow by few percent which is quite negligible with respect to the present uncertainties.

It is important to note that the impact of coalescence cannot be mimicked by heavy quark diffusion, in fact, at variance with it coalescence leads to an enhancement of both $R_{\rm AA}(p_T)$ and $v_2(p_T)$. At RHIC energy, considering coalescence plus fragmentation as the charm quark hadronization mechanism,

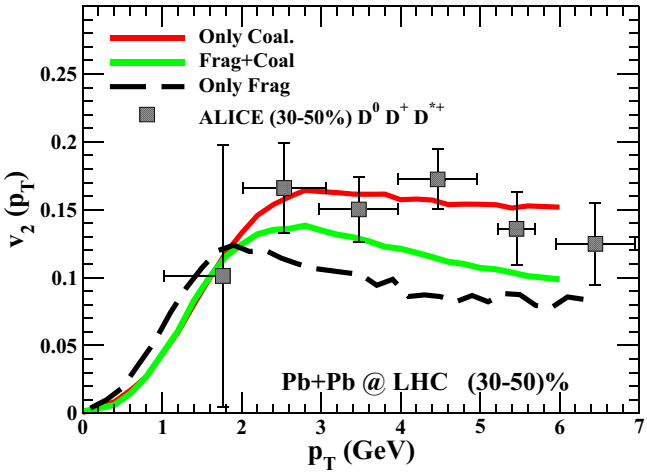

FIG. 11. D meson elliptic flow in $Pb+Pb$ collisions at $\sqrt{s} = 2.76$ ATeV and centrality 30–50% compared to ALICE data. Experimental data has been taken from Ref. [63].

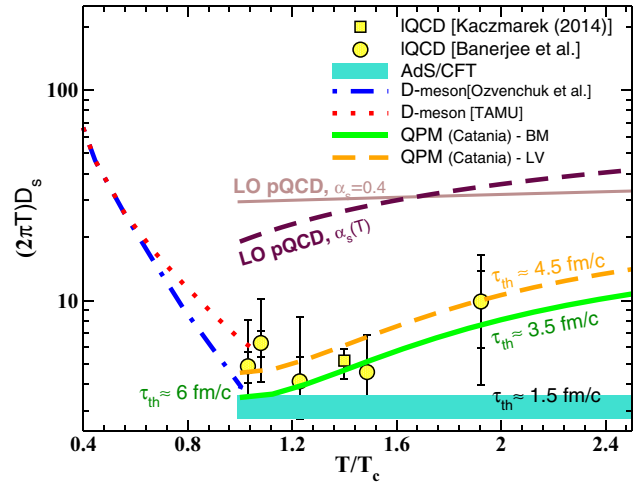

FIG. 12. Spatial diffusion coefficient as a function of temperature obtained within the Boltzmann transport approach and Langevin dynamics to describe experimental data, along with the results from lattice QCD. We have also shown the results obtained within other models. Spatial diffusion coefficient for the QPM model employed to prediction for R_{AA} and v_2 within a Boltzmann (BM) dynamics (green solid line) and with a Langevin (LV) one (orange dashed line) [30]; by symbols quenched lQCD [73] (circles) [74] (square); model calculations based on LO pQCD [11,12] (solid and dashed brown lines) and AdS/CFT rescaled to match the energy density of QCD plasma [71]; in dotted line is shown the D_s coefficient for D meson in hadronic matter [67].

the D meson get about 30% of v_2 from the light partons as a consequence of coalescence. But still the major part of the D meson v_2 (about 65−70%) is coming from the heavy quark diffusion within QGP (heavy quark-bulk interaction). On the other at LHC energy the D meson get about 20−25% v_2 from the light partons as a consequence of coalescence where as about 75−80% is coming from the heavy quark diffusion within QGP (heavy quark-bulk interaction). We remind that the T dependence of the drag coefficient is very important, as pointed out in Ref. [30], to obtained the charm quark flow coming from diffusion.

V. TRANSPORT DIFFUSION COEFFICIENTS AND THERMALIZATION TIME

The space diffusion coefficient D_s is the most significant transport parameter that quantifies the interaction of heavy quarks with the medium that is directly related to the thermalization time and can be evaluated also in lattice QCD, whose more recent calculations are shown by circles and squares in Fig. 12, where a standard quantification of the space diffusion coefficient is done in terms of the a dimensional quantity $2\pi T D_s$. In Fig. 12, we also show T dependence of the spatial diffusion coefficient underlying the predictions for $R_{AA}(p_T)$ and $v_2(p_T)$ described in the previous section. The space diffusion obtained with Boltzmann equation is plotted by green solid line and the one about 30% larger corresponding to the Langevin simulations.

For comparison we also show results obtained within LO pQCD for constant coupling, $\alpha_s = 0.4$, by solid brown line which is independent of temperature. The case with a running coupling $\alpha_s(T)$, maroon solid line, leads to a weak temperature dependence. However, it is well known that such a value of the pQCD D_s cannot describe at all the small $R_{AA}(p_T)$ observed as well as the $v_2(p_T)$. Indeed, from a more rigorous theoretical point of view it has been shown that for charm quarks the perturbative expansion does not show any sign of convergence [66] (unless one is in the weak coupling regime $\alpha_s < 0.05$), and the value shown is only indicative of a LO term. Both lattice QCD and the phenomenology discussed here, as in all other approaches cited in the introduction, firmly agree with a D_s is much smaller than this LO pQCD estimate. In the same plot, we have also shown the results for D meson in the hadronic phase by dotted line the results of Ref. [67], which are also very similar to Refs. [68,69] and by dash dotted line the one in Ref. [70]. The D_s is directly related to the drag coefficient γ driving the HQ in medium evolution that has been discussed in Sec. II. We have $D_s = T/M * \gamma(p \to 0)$ and has to be noticed that in kinetic theory one, and on a more general ground, γ is expected to be proportional to M, hence D_s should be about mass independent providing a general measure of the QCD interaction. It is interesting to estimate the thermalization time, $\tau_{th} \equiv \gamma^{-1}(p \to 0)$, for charm quarks,

$$\tau_{th} = \frac{M}{2\pi T^2}(2\pi T D_s) \cong 1.8 \frac{2\pi T D_s}{(T/T_c)^2} \text{ fm/c}, \qquad (10)$$

where we have substituted a charm quark mass $M = 1.4$ GeV and we have written τ_{th} in terms of a dimensional quantities to facilitate a direct evaluation. For example, at $T \simeq 2\,T_c$ the dashed orange lane as the central value of lQCD gives $2\pi T D_s = 10$, which means a $\tau_{th} \simeq 4.5$ fm/c as indicated directly in the figure. Similarly, one can easily derive the values in the other points of the plot, in the QGP branch. Notice that none of the behavior shown corresponds to a constant thermalization time which would imply a drag γ completely T-independent; i.e., $2\pi T D_s \propto T^2$. In particular, the flat $2\pi T D_s$ corresponds to a thermalization time proportional to $1/T^2$

which is the case of AdS/CFT [71] and pQCD with constant coupling.

The predictions relative to R_{AA} and v_2 obtained by means of the Boltzmann equation with the QPM model indicate a thermalization time that stays in the the range 3.5–6 fm/c which at LHC energy is smaller then the lifetime of the QGP, especially in central collisions. However, it has been noticed in Ref. [72] that the $R_{AA}(p_T)$ still significantly deviates, also at low p_T smaller than 3–4 GeV, from the one expected in case of full thermalization. This is an aspect that has to be investigated in more details to spot the origin of such a deviation. However, it has to be considered that our estimate of thermalization time is done in the $p \to 0$ limit, should take into account for the decreasing of the interaction with the increasing of the momentum which implies a thermalization time of about a 50% larger or more, once average over momentum is done.

We also mention that the $2\pi T D_s$ estimated in the Langevin case, orange dashed line, is nearly identical to the one of the T-matrix approach [34], while the Boltzmann one is quite close to the one from the PHSD transport approach which is based indeed on a dynamical quasiparticle model that includes also finite widths [31].

It may be mentioned that our D_s is marginally below the lattice QCD data point near T_c. A final assessment requests in principle the inclusions of initial state fluctuations [40,75], which helps to develop a large suppression than the averaged one, but such an effect is in practice quite nominal pointing to a somewhat smaller drag coefficient, hence, a larger D_s. Such an effect is expected to be within a 10%. Also as shown in Refs. [76,77], the pre-equilibrium phase may affect the heavy quark suppression pointing also to a somewhat larger D_s for a better agreement with data from the experiments. However, the impact of these further aspects is in general less relevant with respect to the differences between Langevin and Boltzmann approaches and quite smaller than current experimental error bars and the systematic uncertainties in lattice QCD calculations. Certainly, we are reaching a stage where it will become relevant to include them, especially with the upcoming experimental data expected with much smaller error bars and the new data on the triangular flow v_3 [78–80] that, however, is beyond the scope of the present paper. Certainly, our work gives a further contribution in showing that the extraction of the diffusion coefficient from the phenomenology of heavy-ion collisions is possible and reliable.

VI. SUMMARY AND CONCLUSIONS

We have studied the heavy quark propagation in QGP at RHIC and LHC within a Boltzmann transport approach. We start with a charm quark initialization describing the D mesons production in $p+p$ collisions reasonable well at both RHIC and LHC energies within an hadronization by independent fragmentation. The heavy quark and the bulk interaction has been taken into account within a QPM, which is able to reproduce the lattice QCD equation of state and their in-medium evolution has been treated with a Boltzmann transport equation with some comparison to the Langevin one. The hadronization of heavy quark in AA collisions is described by means of a hybrid model of fragmentation plus coalescence. Using the same interaction, we have calculated the R_{AA} and v_2 of heavy meson at different centrality class as well as different colliding energies. Our model gives a good description for D meson R_{AA} and v_2 both at RHIC and LHC within the still significantly large systematic and statistical uncertainties. There are three main ingredients that we identify as playing a key role toward the agreement to the experimental data. The first one is the QPM that enhances the heavy quark bulk interaction near T_c with respect to a mere decrease of the drag coefficient γ with $1/T^2$. This nonperturbative behavior caught by a QPM modeling fitted to the lattice QCD thermodynamics was identified as the key ingredient for the build-up of a large v_2 [30] in a Langevin approach and is confirmed within the Boltzmann approach mainly discussed in the present paper.

Implementation of heavy quark hadronization by means of a hybrid model of fragmentation plus coalescence help to increase both the R_{AA} and v_2 close to the data, if the coalescence is regulated to exhaust hadronization in the zero momentum region, the effect is quite large and essential. Finally as discussed in Ref. [35] for test calculations and ideal cases, once the interaction is tuned to very similar $R_{AA}(p_T)$ the Boltzmann approach is more efficient in reproducing the elliptic flow with respect to Langevin an effect that for the QPM model is of about a 15%.

The underlying $2\pi T D_s$ diffusion coefficient rises about linearly with temperature T and leads to an initial thermalization time of about 3 fm/c at the maximum initial temperature reached at LHC energy ($T \simeq 3T_c$) increasing only to about a 6 fm/c around T_c. This would suggest that the core of charm quarks produced may be essentially kinetically thermalized at the time where most hadronization occurs. A finding that was certainly unexpected before starting the endeavor to study heavy quark diffusion in the quark gluon plasma and that can have important implications for the understanding also of the quarkonia production.

It may be mentioned here that the hadronic rescattering, while generally not strongly affecting R_{AA}, give a further contribution to D meson v_2 that is in the range of 10−20% [64,65], depending on the T_c assumed that is generally in the range 155–175 MeV. Considering the fact that we use T_c=155 MeV, our results on R_{AA} will not be affected significantly by the hadronic rescattering, even if in general a large v_2 is build-up [64,65]. In any case, hadronic rescattering would lead to an improvement of the agreement between the experimental data and the present modeling.

Our result and the estimated $D_s(T)$ shows nice agreement with lattice QCD data within the still significantly large uncertainties. This feature is shared nowadays by most of the modelings, as discussed in Ref. [7]; in particular, our estimate of the value and T dependence of $D_s(T)$ is quite close to Refs. [31,34]. Even if it should be quantified if also the agreement to the data is quantitatively similar. Other approaches can lead to a current estimate that indicates similar values but with a weaker temperature dependence. In general, this can be traced back to some difference in the evolution of the bulk matter and/or to a different impact of coalescence. However, especially for this last point upcoming data on Λ_c/D and D_s/D will shed a new light and allow for more stringent

constraints on the hadronization mechanism. Therefore, in the next future it would be important that all the phenomenological approaches aiming at the evaluation of the heavy transport coefficient provide their predictions also for such ratios as a function of transverse momentum. Furthermore, we think that we are reaching a stage where starts, to be appropriate, to have a comparison to several experimental data as a function of energy and centrality that is statistical quantified. This effort has already been started by some groups [81], but it will also be more meaningful and powerful with the new upcoming data that are expected to carry much smaller error bars and to be extended to lower p_T, the region more relevant for the transport coefficient determination. Given that current uncertainties in the phenomenological approach are comparable if not smaller than the current lattice QCD data, it is desirable that in the following years the latter will be able to reduce the present systematic uncertainties. Certainly, open heavy flavor physics in ultrarelativistic heavy-ion collisions is showing to really have the potential to link the phenomenology to lattice QCD for studying the transport properties of the Hot QCD matter.

ACKNOWLEDGMENTS

We acknowledge the support by the ERC StG under the QGPDyn Grant No. 259684. V.G. acknowledge also the warm hospitality at the UCAS in Beijing under the President International Fellowship Initiative (Grant No. 2016VMA063).

[1] E. V. Shuryak, Nucl. Phys. A **750**, 64 (2005).
[2] B. V. Jacak and B. Muller, Science **337**, 310 (2012).
[3] R. Rapp and H. van Hees, in *Quark Gluon Plasma 4*, edited by R. C. Hwa and X. N. Wang (World Scientific, Singapore, 2010), pp. 111–206.
[4] A. Andronic *et al.*, Eur. Phys. J. C **76**, 107 (2016).
[5] F. Prino and R. Rapp, J. Phys. G **43**, 093002 (2016).
[6] G. Aarts *et al.*, Eur. Phys. J. A **53**, 93 (2017).
[7] V. Greco, Nucl. Phys. A **967**, 200 (2017).
[8] A. Adare *et al.* (PHENIX Collaboration), Phys. Rev. Lett. **98**, 172301 (2007).
[9] B. I. Abeleb *et al.* (STAR Collaboration), Phys. Rev. Lett. **98**, 192301 (2007).
[10] S. S. Adler *et al.* (PHENIX Collaboration), Phys. Rev. Lett. **96**, 032301 (2006).
[11] H. van Hees and R. Rapp, Phys. Rev. C **71**, 034907 (2005).
[12] G. D. Moore and D. Teaney, Phys. Rev. C **71**, 064904 (2005).
[13] H. van Hees, V. Greco, and R. Rapp, Phys. Rev. C **73**, 034913 (2006).
[14] H. van Hees, M. Mannarelli, V. Greco, and R. Rapp, Phys. Rev. Lett. **100**, 192301 (2008).
[15] V. Greco, C. M. Ko, and R. Rapp, Phys. Lett. B **595**, 202 (2004).
[16] V. Greco, C. M. Ko, and P. Levai, Phys. Rev. Lett. **90**, 202302 (2003).
[17] P. B. Gossiaux and J. Aichelin, Phys. Rev. C **78**, 014904 (2008).
[18] W. M. Alberico *et al.*, Eur. Phys. J. C **71**, 1666 (2011); **73**, 2481 (2013).
[19] S. Plumari, W. M. Alberico, V. Greco, and C. Ratti, Phys. Rev. D **84**, 094004 (2011).
[20] H. Berrehrah, P. B. Gossiaux, J. Aichelin, W. Cassing, and E. Bratkovskaya, Phys. Rev. C **90**, 064906 (2014).
[21] S. Cao and S. A. Bass, Phys. Rev. C **84**, 064902 (2011).
[22] S. Cao, G.-Y. Qin, S. A. Bass, and B. Müller, Nucl. Phys. A **904**, 653c (2013).
[23] S. Cao, T. Luo, G. Y. Qin, and X. N. Wang, Phys. Rev. C **94**, 014909 (2016).
[24] M. Djordjevic and M. Djordjevic, Phys. Lett. B **709**, 229 (2012).
[25] P. B. Gossiaux, J. Aichelin, T. Gousset, and V. Guiho, J. Phys. G **37**, 094019 (2010).
[26] S. K. Das, J.-E. Alam, and P. Mohanty, Phys. Rev. C **82**, 014908 (2010).
[27] M. Djordjevic and M. Djordjevic, Phys. Lett. B **734**, 286 (2014).
[28] Z. B. Kang, F. Ringer, and I. Vitev, J. High Energy Phys. 03 (2017) 146.
[29] J. Uphoff, F. Senzel, O. Fochler, C. Wesp, Z. Xu, and C. Greiner, Phys. Rev. Lett. **114**, 112301 (2015).
[30] S. K. Das, F. Scardina, S. Plumari, and V. Greco, Phys. Lett. B **747**, 260 (2015).
[31] T. Song, H. Berrehrah, D. Cabrera, W. Cassing, and E. Bratkovskaya, Phys. Rev. C **93**, 034906 (2016).
[32] J. Liao and E. Shuryak, Phys. Rev. Lett. **102**, 202302 (2009).
[33] F. Scardina, M. di Toro, and V. Greco, Phys. Rev. C **82**, 054901 (2010).
[34] M. He, R. J. Fries, and R. Rapp, Phys. Rev. Lett. **110**, 112301 (2013).
[35] S. K. Das, F. Scardina, S. Plumari, and V. Greco, Phys. Rev. C **90**, 044901 (2014).
[36] G. Ferini, M. Colonna, M. di Toro, and V. Greco, Phys. Lett. B **670**, 325 (2009); V. Greco, M. Colonna, M. di Toro, and G. Ferini, Progr. Part. Nucl. Phys. **62**, 562 (2009).
[37] M. Ruggieri, F. Scardina, S. Plumari, and V. Greco, Phys. Rev. C **89**, 054914 (2014).
[38] S. Plumari, A. Puglisi, F. Scardina, and V. Greco, Phys. Rev. C **86**, 054902 (2012).
[39] M. Ruggieri, F. Scardina, S. Plumari, and V. Greco, Phys. Lett. B **727**, 177 (2013).
[40] S. Plumari, G. L. Guardo, F. Scardina, and V. Greco, Phys. Rev. C **92**, 054902 (2015).
[41] S. Borsanyi, G. Endrodi, Z. Fodor, A. Jakovac, S. D. Katz, S. Krieg, C. Ratti, and K. K. Szabo, J. High Energy Phys. 11 (2010) 077.
[42] S. Plumari, G. L. Guardo, V. Greco, and J. Y. Ollitrault, Nucl. Phys. A **941**, 87 (2015).
[43] P. Romatschke and U. Romatschke, Phys. Rev. Lett. **99**, 172301 (2007).
[44] H. Song, S. A. Bass, U. Heinz, T. Hirano, and C. Shen, Phys. Rev. C **83**, 054910 (2011); **86**, 059903 (2012).
[45] B. Schenke, S. Jeon, and C. Gale, Phys. Rev. C **82**, 014903 (2010).
[46] H. Niemi, G. S. Denicol, P. Huovinen, E. Molnar, and D. H. Rischke, Phys. Rev. Lett. **106**, 212302 (2011).
[47] H. Berrehrah, E. Bratkovskaya, W. Cassing, P. B. Gossiaux, J. Aichelin, and M. Bleicher, Phys. Rev. C **89**, 054901 (2014).
[48] V. Greco, C. M. Ko, and P. Lévai, Phys. Rev. C **68**, 034904 (2003).

[49] T. Lang, H. van Hees, J. Steinheimer, Y. P. Yan, and M. Bleicher, J. Phys. Conf. Ser. **426**, 012032 (2013).
[50] T. Lang, H. van Hees, G. Inghirami, J. Steinheimer, and M. Bleicher, Phys. Rev. C **93**, 014901 (2016).
[51] C. Peterson, D. Schlatter, I. Schmitt, and P. M. Zerwas, Phys. Rev. D **27**, 105 (1983).
[52] K. J. Eskola, H. Paukkunen, and C. A. Salgado, J. High Energy Phys. 04 (2009) 065.
[53] B. Abelev *et al.* (ALICE Collaboration), J. High Energy Phys. 09 (2012) 112.
[54] L. Adamczyk *et al.* (STAR Collaboration), Phys. Rev. D **86**, 072013 (2012).
[55] M. Cacciari, P. Nason, and R. Vogt, Phys. Rev. Lett. **95**, 122001 (2005).
[56] M. Cacciari, S. Frixione, N. Houdeau, M. L. Mangano, P. Nason, and G. Ridolfi, J. High Energy Phys. 10 (2012) 137.
[57] H. Song and U. W. Heinz, Phys. Rev. C **78**, 024902 (2008).
[58] L. Adamczyk *et al.* (STAR Collaboration), Phys. Rev. Lett. **113**, 142301 (2014).
[59] S. K. Das, S. Plumari, S. Chatterjee, J. Alam, F. Scardina, and V. Greco, Phys. Lett. B **768**, 260 (2017).
[60] M. Nahrgang, J. Aichelin, P. B. Gossiaux, and K. Werner, Phys. Rev. C **93**, 044909 (2016).
[61] L. Adamczyk *et al.* (STAR Collaboration), Phys. Rev. Lett. **118**, 212301 (2017).
[62] J. Adam *et al.* (ALICE Collaboration), J. High Eenergy Phys. 03 (2016) 081.
[63] B. Abelev *et al.* (ALICE Collaboration), Phys. Rev. Lett. **111**, 102301 (2013).
[64] M. He, R. J. Fries, and R. Rapp, Phys. Lett. B **735**, 445 (2014).
[65] S. K. Das, J. M. Torres-Rincon, L. Tolos, V. Minissale, F. Scardina, and V. Greco, Phys. Rev. D **94**, 114039 (2016).
[66] S. Caron-Huot and G. D. Moore, Phys. Rev. Lett. **100**, 052301 (2008).
[67] M. He, R. J. Fries, and R. Rapp, Phys. Lett. B **701**, 445 (2011).
[68] L. Tolos and J. M. Torres-Rincon, Phys. Rev. D **88**, 074019 (2013).
[69] S. K. Das, S. Ghosh, S. Sarkar, and J.-E. Alam, Phys. Rev. D **85**, 074017 (2012).
[70] V. Ozvenchuk, J. M. Torres-Rincon, P. B. Gossiaux, J. Aichelin, and L. Tolos, Phys. Rev. C **90**, 054909 (2014).
[71] S. S. Gubser, Phys. Rev. D **76**, 126003 (2007).
[72] A. Beraudo, A. de Pace, M. Monteno, M. Nardi, and F. Prino, Eur. Phys. J. C **75**, 121 (2015).
[73] D. Banerjee, S. Datta, R. Gavai, and P. Majumdar, Phys. Rev. D **85**, 014510 (2012).
[74] O. Kaczmarek, Nucl. Phys. A **931**, 633 (2014).
[75] S. Cao, Y. Huang, G. Y. Qin, and S. A. Bass, J. Phys. G **42**, 125104 (2015).
[76] S. K. Das, M. Ruggieri, F. Scardina, S. Plumari, and V. Greco, J. Phys. G: Nucl. Part. Phys. **44**, 095102 (2017).
[77] S. K. Das, M. Ruggieri, S. Mazumder, V. Greco, and J. E. Alam, J. Phys. G **42**, 095108 (2015).
[78] M. Nahrgang, J. Aichelin, S. Bass, P. B. Gossiaux, and K. Werner, Phys. Rev. C **91**, 014904 (2015).
[79] M. Nahrgang, J. Aichelin, P. B. Gossiaux, and K. Werner, J. Phys. Conf. Ser. **668**, 012024 (2016).
[80] C. A. G. Prado, J. Noronha-Hostler, A. A. P. Suaide, J. Noronha, M. G. Munhoz, and M. R. Cosentino, arXiv:1611.02965.
[81] Y. Xu, M. Nahrgang, J. E. Bernhard, S. Cao, and S. A. Bass, arXiv:1704.07800.
[82] T. Song, H. Berrehrah, E. L. Bratkovskaya, D. Cabrera, W. Cassing, T. Tolos, and J. M. Torres-Rincon, J. Phys. Conf. Ser. **779**, 012030 (2017).